Passive interferometric interrogation of a magnetic field sensor using an erbium doped fiber optic laser with magnetostrictive transducer

I.M. Nascimento[a,b,*], J.M. Baptista[a,c], P.A.S. Jorge[a,b], J.L. Cruz[d], M.V. Andrés[d]

[a] *INESC TEC, Rua do Campo Alegre, 687, 4169-007 Porto, Portugal*
[b] *Department of Physics and Astronomy, Faculty of Sciences of University of Porto, Rua do Campo Alegre 687, 4169-007 Porto, Portugal*
[c] *Centro de Competências de Ciências Exatas e de Engenharia, Universidade da Madeira, Funchal, Portugal*
[d] *Department of Applied Physics and Electromagnetism, University of Valencia, Spain*
[*] Corresponding author.

Abstract: An erbium doped (Er^{3+}) fiber optic laser is proposed for magnetic field measurement. A pair of FBGs glued onto a magnetostrictive material (Terfenol-D rod) modulates the laser wavelength operation when subject to a static or a time dependent magnetic field. A passive interferometer is employed to measure the laser wavelength changes due to the applied magnetic field. A data acquisition hardware and a LabVIEW software measure three phase-shifted signals at the output coupler of the interferometer and process them using two distinct demodulation algorithms. Results show that sensitivity to varying magnetic fields can be tuned by introducing a biasing magnetic field. A maximum error of 0.79% was found, for magnetic fields higher than 2.26 mT_{RMS}.

1. Introduction

Fiber optic magnetic field sensors have been studied over the years. Special interest has been shown in the high power industry owing to its intrinsic insulation (silica), immunity to electro- magnetic interference, high dynamic range and bandwidth and possibility to employ remote interrogation [1]. Several sensing mechanisms such as magnetic fluid, Lorentz force, Faraday effect and magnetostrictive effect have been proposed for magnetic field measurement. These methods can be used with both constant and varying magnetic fields.

The first mechanism was explored by combining the magnetic fluid with an optical fiber refractive index sensor. In the presence of the magnetic field the refractive index of the fluid changes 3×10^{-4} RIU/mT (RIU: Refractive Index Units) at 28 °C from 0 to 70 mT [2].

Sensors established on the Lorentz force require another current carrying conductor (few milliamps) that will experience deformation in the presence of an orthogonal magnetic field. Although they do not experience hysteresis, the deformation induced is very small; in [3] the optical sensor is a Distributed feedback laser, with a Pi-Shift FBG written in Er^{3+} fiber, and the wavelength changes are read with a Michelson interferometer with 25 m of optical path imbalance. A minimal detected field of 1.5 $\mu T/Hz^{1/2}$ was calculated. Another alternative reported consists on using a 6 cm long cavity laser with one longitudinal mode and two orthogonal polarizations. Measurement of the beat frequency between these two polarizations is proportional to the laser birefringence and changes according to pressure exerted in the cavity due to the Lorentz force. Results showed relatively good linearity for magnetic fields between 4 and 20 mT [4].

Faraday effect is one of the most popular optical sensing mechanisms for magnetic field. It consists of light polarization rotation induced by the magnetic field as it propagates through a sensing medium and its sensitivity depends on the medium Verdet constant. While standard fiber optic can be used as a sensing medium to observe the Faraday effect, the Verdet constant of silica is very small and the wounding of the fiber around the conductor gives rise to linear birefringence, further degrading the sensitivity [5]. A prototype operating at 850 nm and based on a Sagnac configu- ration was developed and tested where a maximum errorof 0.2% was achieved for currents ranging from 300 to 4000 A_{RMS} and temperatures from 40 °C up to 60 °C, satisfying 0.5 class operation [6]. Faraday based sensors are affected by the residual birefringence of standard fibers [7], although this problem has been recently overcomed in standard fibers [8], an alternative solution has been

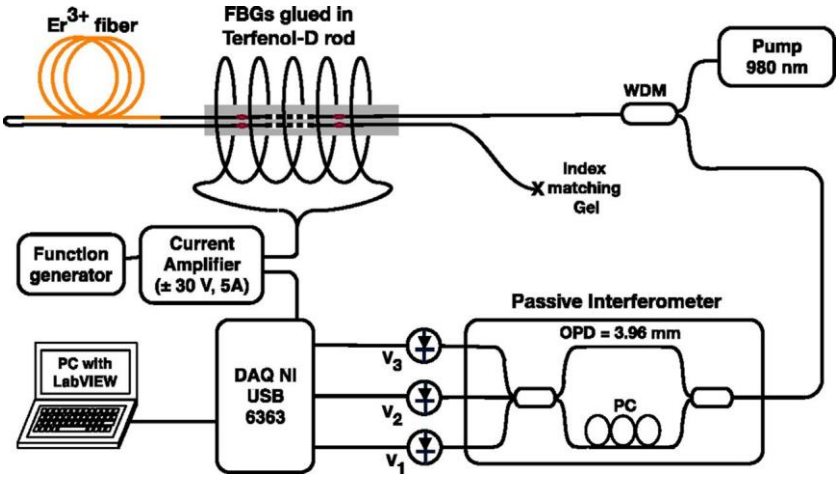

Fig. 1. Experimental setup including the laser, passive interferometer and acquisition setup.

the use of spun fibers of low birefringence or high circular birefringence [9,10]. On the other hand, the bulk glass materials are more robust and can have higher Verdet constants than fibers. However, fiber alignment with the bulk material is tricky [11,12]. In [11] a sensor operating at 820 nm in a close loop configuration achieved a 5.5% error under stable environmental conditions from 10 A–20 kA.

In the last category, magnetostricitve elements can be deposited or glued to an optical fiber strain sensor. In reference [13], Terfenol- D is deposited in an etched FBG (Fiber Bragg Grating) with 86 μm diameter, improvingthe sensitivity from 0.386 to 0.95 pm/mT. A distributed sensor was also developed in [14] and consists in wounding a standard single mode fiber around a nickel wire. In the presence of the magnetic field the nickelwire stretches and the phase of the Rayleigh backscattered light changes according to it. A passive Mach– Zehnder interferometer with a 3 3 coupler and an OPD of 2 m (1 m spatial resolution) was used to read the phase changes.

In this paper we present an erbium doped optical fiber laser with two FBGs whose wavelength is modulated according to the external magnetic field. The transducer element is a Terfenol-D rod that stretches both FBGs, changing the laser emission wavelength. This variation is converted into an intensity modulation at the output of a passive interferometer using a 3 3 output coupler. The laser combines higher SNR (Signal to Noise Ratio) with narrower band- width, enabling, together with the interferometric readout system, a higher resolution than is attainable with systems based on the direct modulation of a single FBG.

2. Principle

The implemented setup is demonstrated in Fig. 1. The laser consists of two FBGs at 1534.17 nm with 150 pm spectral width (at half power) and 82% reflectivity, and the other at 1534.21 nm with 160 pm spectral width and 87% reflectivity, written in single mode Boron codoped Photosensitive fiber using a 1058 nm period phase mask. In between the two FBGs, a piece of 6.8 m of Fibercore Erbium doped fiber M-5 is used as the gain medium, resulting in 8 m cavitylength.

Each FBG is glued side by side in two points, distant 2 cm apart, in a Terfenol-D (composition $Tb_{0.27}Dy_{0.73}Fe_2$) rod having a diameter of 0.5 cm and 10 cm in length. The thickness of the material limits the magnetic field frequency response to 100 kHz. A function generator, a current amplifier and an inductor are used to generate magnetic field (AC and/or DC with a magnetic-current relation of 12.2 mT/A), modulating both FBGs and consequently the laser wavelength emission. The AC and the DC magnetic field correspond to the alternate and constant field, respectively. Laser operation in reflection is preferable than in transmission as no residual pump power is present in the output.

For the detection of the magnetic field induced wavelength shift, an interferometric readout scheme was set up. A passive interferometer, having a *OPD* of 3.96 mm (Optical Path Difference) resulting in a spectral range of 594 pm between interferometric fringes at 1534 nm was built with a 2 2 and a 3 3 coupler at the input and output, respectively, producing three outputs with 120 degreesphase difference between them, given by [15]:

$$V_n = A_i + B\,\mathrm{Cos}[\phi(t) + \phi_{DC} - (n-1)2\pi/3] \quad (1)$$

where n is the output 1, 2 and 3, A_i is the DC component obtained when sweeping one period of the interferometer, B is the visibility of the fringes which is maximized by a polarization controller (PC), $\phi(t)$ and ϕ_{DC} is the time varying and DC interferometer phase, respectively. In such configuration, any change in the laser emission wavelength results in a change of the interferometer optical output phase ($\phi(t)$ and ϕ_{DC}) proportional to the OPD. This way, the interferometer acts like a wavelength-to-intensity modulator enabling to track the wavelength changes, induced by the magnetic field, very accurately with low cost instrumentation.

This interferometer has the advantage of not needing an active element to avoid total output fading. The

relative phase of the three outputs and the signal processing can always retrieve the relevant output information, independently of the random drift of the interferometer. Nevertheless, the interferometer drift is mixed with the DC phase changes, also affecting the output intensity and limiting the application of this scheme to AC measurements. In any case, magnetic field measurements were performed in a temperature- controlled environment.

A 16 bits analogue-digital converter from NI (National Instruments) with 305 μV resolution and 2 Mbps bandwidth is used to read the three outputs of the interferometer and the applied current signal to the inductor. In this way, the use of virtual instrumentation becomes possible, making it straightforward to test and implement any signal processing algorithm, by simply adjusting the software, offering a much higher versatility and scalability. There- fore, to test the versatility of virtual instrumentation systems, a LabVIEW program was developed to process the interferometric signals, and used to test and implement, simultaneously, two distinctive demodulation methods. The first one (type I) is presented in Fig. 2 and consists on performing derivatives and an integration as depicted [15]. The output only contains the variant phase information and in order for this method to work properly the values of A_i must be the same for the three outputs, which is achieved by introducing an adjustable gain in each interferometer signal.

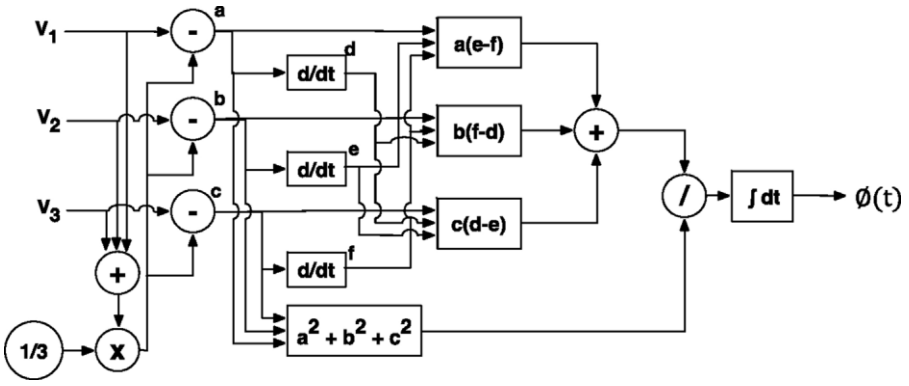

Fig. 2. Type I processing diagram.

The other implemented algorithm (type II) consists on perform- ing the Arc tangent function of the signals provided by the detectors[16]:

$$\phi(t) + \phi_{DC}=\text{Arctan}[3^{1/2}(a_3V_2-a_2V_3)/(a_3V_2+a_2V_3-2a_2a_3V_1)] \quad (2)$$

where $a_2 = A_2/A_1$ and $a_3 = A_3/A_1$. If the three outputs have the same gain then.a_3=1. Although it is possible to recover the continuous phase information, the interferometer drift is also present and this method also requires an unwrapping algorithm to compensate phase changes out of p.

Laser emission wavelength is temperature dependent and it is affected by the FBGs response to temperature and strain induced by the Terfenol-D rod due to thermal expansion. At the output of the interferometer this effect will be mixed with the random drift of the interferometer and using type I method this DC effects are excluded. On the other hand, when using the type II method the output will contain the temperature effect but having a slow variation which is simply removed by filtering the AC response.

3. Results

3.1. Laser

Laser spectral width is measured by coupling a tunable laser (100 kHz bandwidth) with the developed one. In the frequency domain, the convolution of both incoherent signals is read with a 50 GHz photodetector and an Electric Spectral Analyzer. Since the tunable laser is very narrow when compared to the developed laser the result gives the spectral shape of the laser, centered in the frequency given by the beat frequency of both [17]. In Fig. 3 it is shown the laser spectrum obtained with the electrical spectrum analyzer. A spectral width of 1.87 GHz (14.7 pm at 1534 nm) was measured for a pump power of 560 mW, the laser linewidth is 40 times smaller than the fringe spectrum range of the interrogation interferometer assuring adequate sensitivity. The linewidth dependence on pump power is residual and the variations are negligible with respect to the free spectral range of the interferometer, the slight benefits of the linewidth reduction are partially faded by the reduction of the emitted power, therefore, the pump level had little impact on the sensor performance. During the following measurements, the pump power was set at 560 mW.

Using the Thorlabs PM20CH power meter the laser response was characterized using several pump power levels. Fig. 4 shows a maximum laser power of 4.7 mW for 560 mW pump and a threshold of 50 mW for lasing.

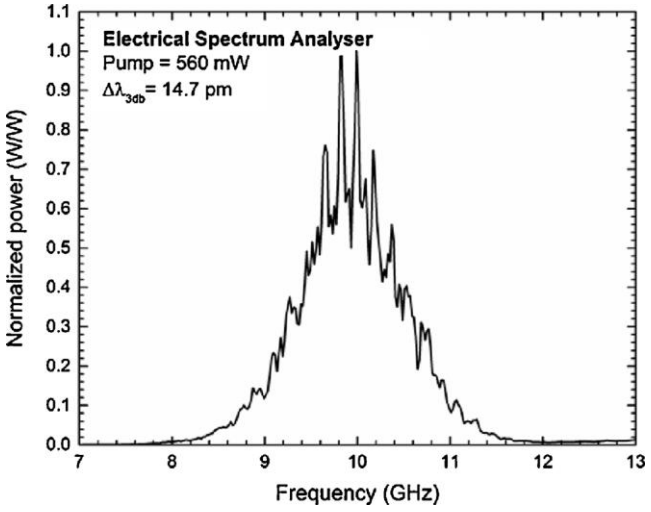

Fig. 3. Laser spectrum measured in an electrical spectral analyzer.

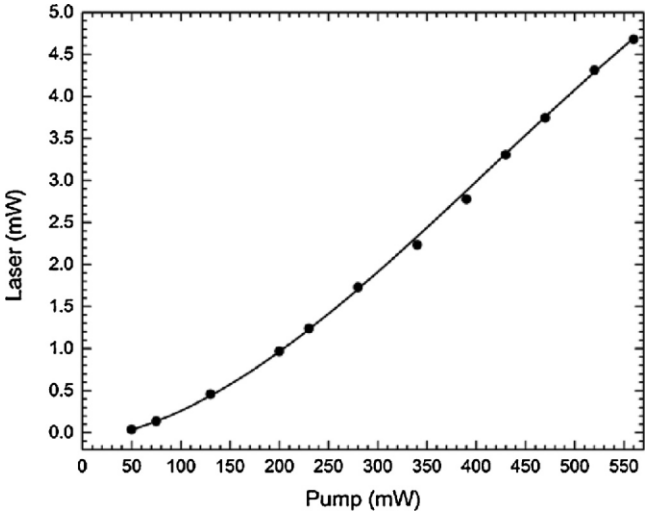

Fig. 4. Laser power in function of the pump power.

Laser power stability was also measured along the time using a photodetector and the analogue digital converter. Recording the laser power with an acquisition sampling frequency of 10 kHz showed that the laser had an output power modulation below 1.2% at 50 Hz caused by the electronics driving the pump diode. Long term power fluctuations of about 4% where observed as well, how- ever the detection electronics compensates for this slow variation.

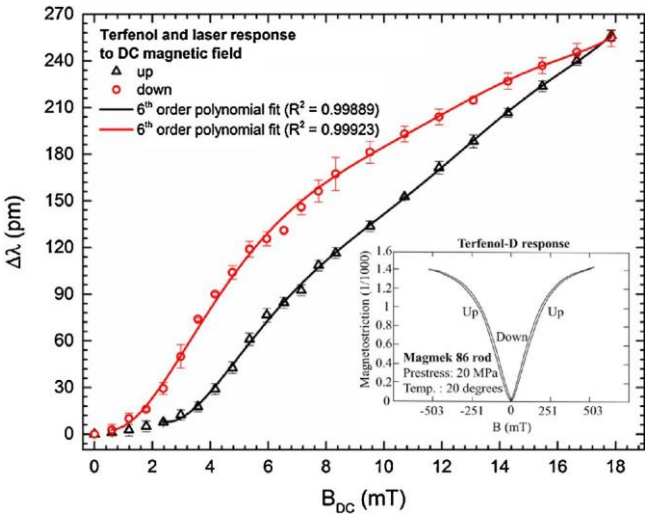

Fig. 5. Laser wavelength change with DC magnetic field and in the inset the material response according to the manufacture.

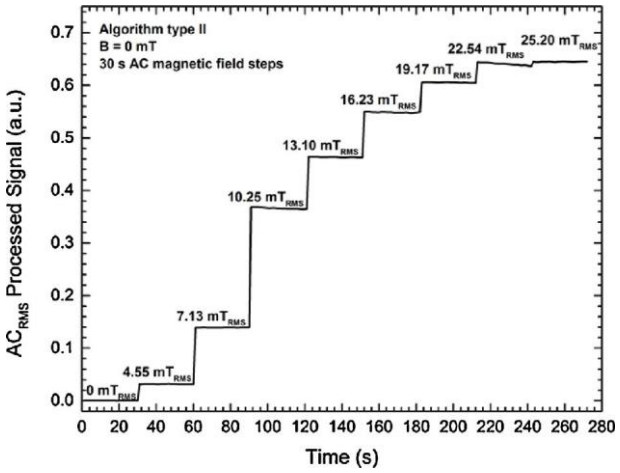

Fig. 6. Steps of AC magnetic fields with 0 mT offset.

3.2. Magnetic field measurement

Several continuous current steps were applied to the coil and the laser wavelength changes were recorded using a wavelength meter Burleigh WA-1650 (0.5 pm resolution). Fig. 5 shows the magnetostrictive response of Terfenol-D driving the laser emission wavelength, the hysteresis cycle was obtained with three independent tests when the magnetic field goes up and down. The error bars correspond to the standard deviation of the three independent measurements, and account for the repeatability of the sensor, or the measurement precision. The maximum fluctuation registered was of 4.5 pm at B = 5.95 mT for the up curve and 10.7 pm at B = 8.33 mT for the down curve. In all cases, the measurement accuracy, given by the deviation between the measurement points and the non-linear calibration curve was much better, corresponding to smaller error values. The non-linear behavior of the calibration curve is intrinsic to the Terfenol-D response to DC magnetic fields, as can be seen in the inset of Fig. 5, where a representation of the manufacturer Data-sheet is given (notice that an unloaded rod was used, therefore saturation is reached with an applied field smaller than the one presented in the inset of Fig. 5). The material expansion in the presence of a magnetic field is non-linear and independent of the negative and positive sign of the magnetic fields. Therefore, when no bias magnetic field is applied, the application of an AC magnetic field results in a response that is doubled in frequency. Moreover, since the transducer is intrinsically non-linear, different DC biasing points will result in different sensitivities to AC fields. Hysteresis is an additional problem for DC measurements that is overcame with specific setups [18].

The laser response to alternate magnetic fields (AC) at 20 Hz was characterized using different constant magnetic fields (DC), with the setup presented in Fig. 1. The acquisition system was defined with 10 kHz sample frequency and a low pass filter with 200 Hz cut- off was applied for each input signal, before processing the three outputs of the interferometer. The AC RMS value was obtained after filtering the demodulated signal with a second order Butterworth band-pass filter with a 5 Hz bandwidth.

Fig. 6 shows the RMS AC response for a DC magnetic field of 0 mT applying different AC steps during 30 s each. The results were obtained with the demodulation process type II and the values shown in each step correspond to the average value. Response of the Terfenol-D to positive and negative magnetic fields is the same. So for 0 mT magnetic field offset, the AC magnetic field pro-

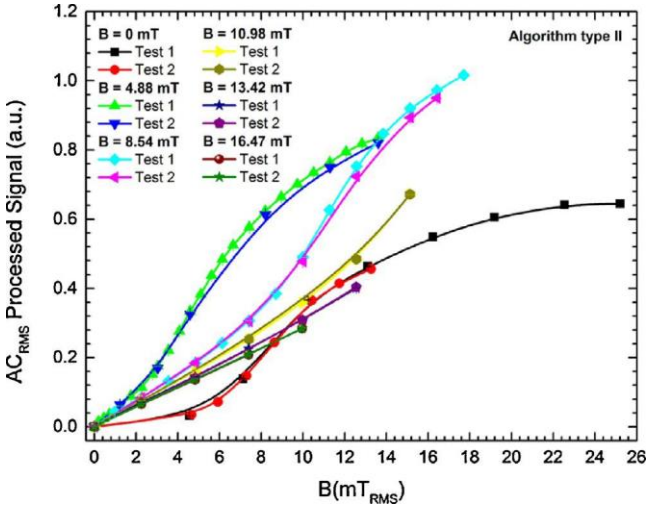

Fig. 7. Type II demodulation algorithm response to AC, using different magnetic field offsets.

duces a modulation whose frequency is acquired at two times the modulation frequency. Still when a magnetic field offset is intro- duced the modulation is therefore obtained at the same modulation frequency. Taking this effect into account, the acquisition will be acquired at to two times the modulation frequency when no bias magnetic field is present or at the modulation frequency when a bias field is applied. In Fig. 6 it is shown that for alternate magnetic fields below 4.55 mT_{RMS} the sensitivity is small, on the other hand, at values higher than 22.54 mT_{RMS} it saturates.

Compilation of the sensor response obtained using demodula tion algorithm type II with different DC magnetic fields is present in Fig. 7. For each, two independent tests were conducted and the results showedgood agreement. Also, a standard deviation error in each step is present, but they are too small to be observed in the plot. Analyzing these results we see that controlling the DC magnetic field offset (this could also be done by a permanent magnet) higher sensitivity can be obtained, depending of the measurement range. For magnetic fields up to 12.2 mT_{RMS} a constant field of 4.88 mT gives the best response. On the other hand, for values higher than 12.2 mT_{RMS}, a DC magnetic field of 8.54 mT is preferable, measuring fields up to 18.2 mT_{RMS}. Moreover the worst sensitivities were found for a constant magnetic field of 0, 13.42 and 16.47 mT, which also corresponded to the worst sensitivity region in Fig. 5.

Table 1
Maximum AC detection errors in percentage obtained with different bias magnetic fields for variant magnetic fields higher than 2.25 mTRMS.

Bias field B (mT)	0.00	4.88	8.54	10.98	13.42	16.47
Type I (%)	1.609	0.406	0.645	0.776	0.655	0.792
Type II (%)	1.562	0.413	0.644	0.757	0.652	0.790
Relative Difference (%)	3.018	−1.645	0.098	2.527	0.412	0.228

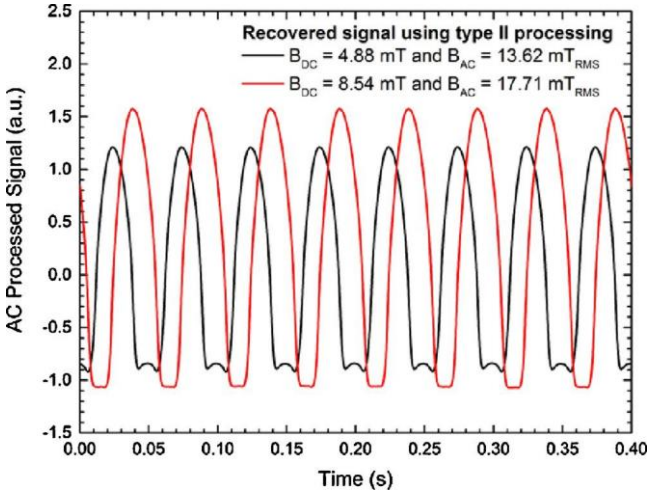

Fig. 8. Type II demodulation AC signals for AC magnetic fields higher than the bias field.

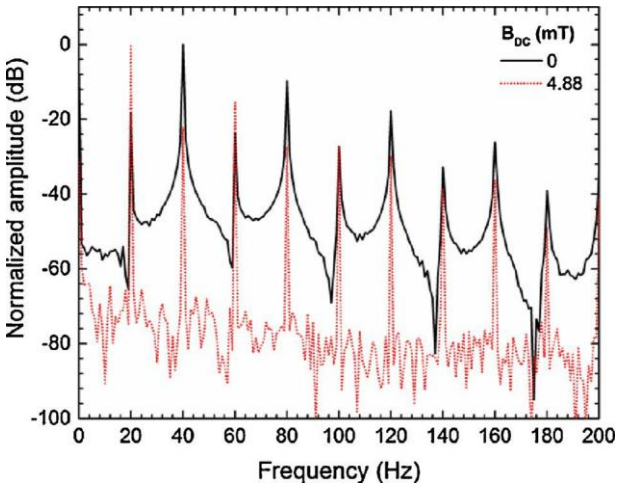

Fig. 9. FTT of the recovered signal at different magnetic fieds.

The same measurements where performed simultaneously with the algorithm I, the plots obtained with the two algorithms where indistinguishable and therefore the results have been numerically compared. Considering the results obtained for each independent test maximum errors were calculated and presented in Table 1. The calculation is done considering two times the standard deviation divided by the average AC value in each step for changing magnetic fields higher than 2.25 mT_{RMS}. A maximum error of 1.61% was found considering a zero magnetic field offset. For other offset values the error is lower than 0.79% because the sensitivity is higher for low AC magnetic fields. Also, both demodulations algorithms were compared. Although the same response was obtained, the errors were slightly lower using type II algorithm, which makes use of the Arc tangent function. However, an isolated case, for a bias of 4.88 mT, type II processing gave a slightly superior error. The maximum and minimum improvement obtained with it was 3.02 and 0.1%, respectively. Better resolutions are in general achieved in type II than in type I method because the latter one employs more complex functions such as derivatives and integration, translating in to increased noise.

Fig. 8 shows the signals recovered for two particular cases, where the AC modulation is higher than the bias field. It clearly shows the fundamental frequency of 20 Hz and a distortion in the lower part of the sinusoidal due to the week response of the magnetostrictive material to low magnetic fields. According to Fig. 5, the region of 0–2 mT (field going down) and from 0 to 3 mT (field going down) shows very little response. This range is about 5 mT and justifies the flat response of the lower part of both curves.

The signal to Noise ratio was also inspected by the FFT (Fast Fourier Transform) of the recovered demodulated signal as a function of the bias field considering 20 Hz modulation and bandwidth. In Fig. 9 it is shown the FFT spectrum for a 0 and 4.88 mT bias fields. The results are also compiled in Fig. 10 for a wider range of bias fields, showing a variation between 63 and 67 dB for non-zero bias fields with no dependence with the applied bias field. However, the SNR decreases significantly, to 46 dB for the 40 Hz harmonic when no bias field is applied.

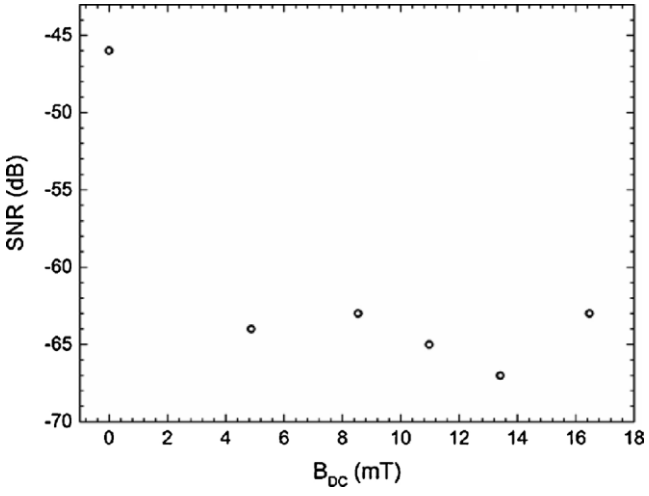

Fig. 10. SNR as a function of the bias field.

In agreement with the DC response of the laser shown in Fig. 5, the best response of the AC current senor is achieved with a low but non-zero biasing field, however the best linearity is obtained for moderate DC fields because the transducer works still far from saturation. These two situations are compared in Fig. 11.

Finally, we have to pint out the foreseeable thermal behav- ior of this system. This sensor is intended for AC measurements, temperature is a quasi-DC effect because of its variation is slow. Temperature has two effects, the first one is the shift of the wave- length emitted by the laser due to the thermal expansion of the transducer, the type I processing of the acquired signals makes up for this shift so that temperature does not affect the measurement of the AC magnetic field, the type II processing can remove the thermal shift by a DC filter. The second thermal effect is the variation of magnetostrictive strain with temperature; although magnetostrictive curves are very sensitive to stress, it has been demonstrated [19,20] that the response of Terfenol-D is almost temperature independent in the range of [0, 90] ºC for excitation fields between 0 and 40 kA/m. Therefore, it is assumed thatthe sensor presented here could be reasonably stable within the temperature ranges and magnetic excitations mentioned before. Thermal calibration would be required beyond these ranges and this is a matter of further analysis.

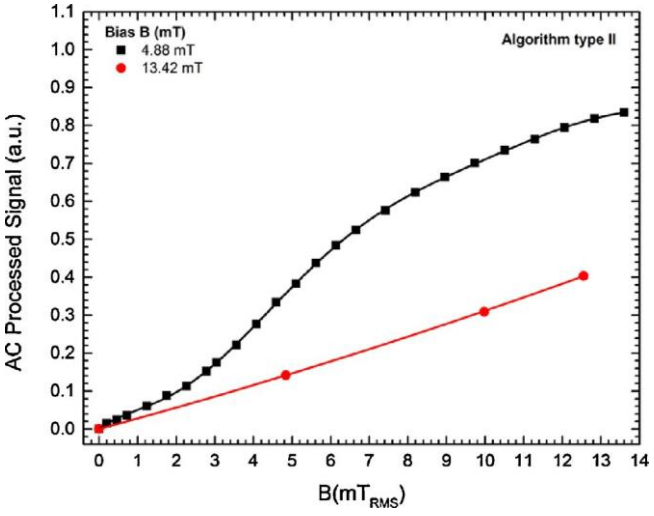

Fig. 11. Type II demodulation algorithm response to AC,

4. Conclusion

A magnetic field sensor based on a fiber optic laser has been proposed. The laser emission wavelength is modulated by a magnetostrictive transducer that stretches the Bragg mirrors of the laser. The sensor is interrogated by a Match–Zener interferometer with three outputs at 120°, the three outputs are processed in real time to retrieve the phase variation induced by the AC wavelength shift giving a stable output. Neither thermal stabilization of the gratings nor drift compensation of the interferometer is required. The response of the sensor to AC magnetic fields has been analysed for different strengths of the DC bias filed; the performance of two different demodulation algorithms has been compared. By tuning the DC magnetic field from 0 to 16.47 mT the AC response showed different responses, where the best sensitivities were achieved for 4.88 and 8.54 mT. Additionally, lower sensitivities were observed when a constant magnetic field of 0, 13.42 and 16.47 mT was applied, corresponding to the lower and higher saturation levels of the magnetostrictive material. Moreover, a maximum error of 0.79% was found for AC magnetic fields above 2.26 mT$_{RMS}$, with a non-zero bias magnetic field. Furthermore, comparison of both demodula- tion algorithms revealed the same response, but errors were lower in all tests when using the arctangent function based algorithm. The maximum and minimum improvement was 3.02% and 0.1%, respectively.

Acknowledgements

This work was supported by project SMARTGRIDS NORTE- 07-0124-FEDER-000056, financed by the North Portugal Regional Operational Program (ON.2-O Novo Norte), under the National Strategic Reference Framework (NSRF), through the European Regional Development Fund (ERDF), and by national funds, through the Portuguese funding agency, Fundação para a Ciência e a Tecnologia (FCT). Ivo Nascimento would like to acknowledge the financial support of FCT (SFRH/BD/80056/2011). J.L. Cruz and M.V. Andrés acknowledge the financial support of the Min- isterio de Economia y Competitividad of Spain, FEDER and Generalitat Valenciana (projects TEC2013-46643-C2-1-R and PROMETEOII/2014/072).

References

[1] H. Cao, N. Shi, J. Xu, A novel design of fiber-optic sagnac current sensor, 2012Fifth Int. Symp. Comput. Intell. Des. (2012) 89–92.

[2] R. Lv, Y. Zhao, D. Wang, Q. Wang, Magnetic fluid-filled optical fiber Fabry–Pérot sensor for magnetic field measurement, IEEE Photonics Technol.Lett. 26 (2014) 217–219.

[3] G.A. Cranch, G.M.H. Flockhart, C.K. Kirkendall, DFB fiber laser magnetic field sensor based on the lorentz force, Opt.

Fiber Sensors (2006) 1–4.

[4] L. Cheng, Z. Guo, J. Han, L. Jin, B. Guan, Ampere force based magnetic field sensor using dual-polarization fiber laser, Opt. Express 21 (2013) 13419– 13424.

[5] P. Drexler, P. Fiala, Utilization of faraday mirror in fiber optic current sensors, Radioengineering 17 (2008) 101–107.

[6] M. Takahashi, K. Sasaki, A. Ohno, Y. Hirata, K. Terai, Sagnac interferometer-type fibre-optic current sensor using single-mode fibre downleads, Meas. Sci. Technol. 15 (2004) 1637–1641.

[7] J.L. Cruz, M.V. Andres, M.A. Hernandez, Faraday effect in standard optical fibers: dispersion of the effective Verdet constant, Appl. Opt. 35 (1996) 922–927.

[8] M. Segura, N. Vukovic, N. White, T. May-Smith, W.-H. Loh, F. Poletti, M.N. Zervas, Low birefringence measurement and temperature dependence in metre-long optical fibers, J. Light. Technol. 8724 (2015) 2015.

[9] D.N. Payne, A.B. Barlow, Development of low and high birefringence optical fibers, Quantum Electron. 18 (1982) 477–488.

[10] N. Peng, Y. Huang, S. Wang, T. Wen, W. Liu, Q. Zuo, L. Wang, Fiber optic current sensor based on special spun highly birefringent fiber, IEEE Photonics Technol. Lett. 25 (2013) 1668–1671.

[11] J. Song, P.G. Mclaren, D.J. Thomson, R.L. Middleton, A faraday effect based clamp-on magneto-optical current transducer for power systems, WESCANEX 95 (1995) 329–333.

[12] N. Fisher, D. Jackson, Vibration immunity for a triangular faraday current sensor, Fiber Integr. Opt. 16 (1997) 321–328.

[13] M. Yang, J. Dai, C. Zhou, D. Jiang, Optical fiber magnetic field sensors with TbDyFe magnetostrictive thin films as sensing materials, Opt. Express 17 (2009) 20777–20782.

[14] A. Masoudi, T.P. Newson, Distributed optical fiber dynamic magnetic field sensor based on magnetostriction, Appl. Opt. 53 (2014) 2833–2838.

[15] D. A. Brown, C.B. Cameron, R.M. Keolian, D.L. Gardner, S.L. Garrett, A symmetric 3×3 coupler based demodulator for fiber optic interferometric sensors, Fiber Opt. Laser Sens. IX 1584 (1991) 328–335.

[16] M. D. Todd, G.A. Johnson, C.C. Chang, Passive light intensity-independent interferometric method for fiber Bragg grating interrogation, Electron. Lett. 35(1999) 1970–1971.

[17] M. Nazarathy, W.V. Sorin, D.M. Baney, S.A. Newton, Spectral analysis of optical mixing measurements, J. Light Technol. 7 (1989) 1083–1096.

[18] D. M. Dagenais, F. Bucholtz, K.P. Koo, A. Dandridge, Detection of low-frequency magnetic signals in a magnetostrictive fiber-optic sensor with suppressed residual signal, J. Light. Technol. 7 (1989) 881–887.

[19] A. E. Clark, High Power Magnetostrictive Transducer Materials-Actuator 92,3rd International Conference on New Actuators, (1992), 127.

[20] E. du, T. de Lacheisserie, D. Gignoux, M. Schlenker, Magnetism: II-material sand applications, magnetostrictive materials, Springer 220 (2002).